JOURNAL OF MATERIALS SCIENCE 20 (1985) 975–988

Use of hydration inhibitors to improve bond durability of aluminium adhesive joints

G. D. DAVIS, J. S. AHEARN, L. J. MATIENZO, J. D. VENABLES
Martin Marietta Laboratories, 1450 South Rolling Road, Baltimore, MD 21227, USA

The adsorption of selected organic hydration inhibitors onto Forest Products Laboratory (FPL)-etched aluminium surfaces and the subsequent hydration of the treated surfaces have been studied using X-ray photoelectron spectroscopy (XPS) and surface behaviour diagrams (SBDs) supplemented by Fourier Transform Infra-red Spectroscopy (FTIR). Wedge tests were used to evaluate performance of these inhibitors in improving bond durability and the locus of failure was identified by XPS and high resolution scanning electron microscopy (X-SEM). The results indicate that nitrilotris methylene phosphonic acid (NTMP) and related compounds adsorb to the alumina surface via the POH bonds of the phosphonic acid groups, resulting in a displacement of water normally adsorbed onto the surface. A model of adsorption was developed which suggests that after treatment with very low concentrations of inhibitor (~ 1 ppm), only one leg of the NTMP molecule adsorbs onto the surface although at higher concentrations (~ 100 ppm) all three legs adsorb. Hydration is a three-step process: (i) reversible physisorption of water; (ii) slow dissolution of the inhibitor followed by rapid hydration of the freshly exposed Al_2O_3 to boehmite (AlOOH); and (iii) further hydration of the AlOOH to bayerite [$Al(OH)_3$]. Analysis of the adsorption, hydration, and wedge test results using different inhibitors suggests the following five inhibitor characteristics that promote good bond performance: (i) displacement of water and occupation of all active sites on the Al_2O_3 surface; (ii) formation of strong inhibitor surface bonds; (iii) insolubility of the resulting inhibitor–aluminium complex in aqueous solutions; (iv) compatibility with the adhesive or primer; (v) coupling of the inhibitor to the adhesive.

1. Introduction

The performance of adhesively bonded aluminium structures is judged primarily by the initial bond strength and the long-term durability of the bond. The high initial bond strength provided by commercial aerospace bonding processes [1, 2] is a consequence of the microscopically rough aluminium oxide formed during the etching or anodization treatment. When polymeric adhesive is added, it penetrates the oxide pores and surrounds the oxide whiskers, resulting in a physical interlocking that ensures a much stronger bond than that possible with a smooth oxide surface [3, 4].

The oxide morphology also partially governs long-term bond durability in moist environments in that the mechanical interlocking of an adhesive and a rough aluminium oxide can maintain high bond strength even if the chemical interaction between the oxide and polymer is diminished. In this case, a crack propagates only if interlocking is destroyed or failure occurs cohesively in that adhesive. In previous work crack propagation occurred as the aluminium oxide hydrated to the oxyhydroxide, boehmite, allowing failure either at the boehmite–metal or boehmite–adhesive interface prior to a cohesive failure in the adhesive, the ultimate performance limit of an adhesive bond [5–7].

These findings have prompted investigations of methods to inhibit the oxide-to-hydroxide conversion process and thereby to improve the long-term

0022–2461/85 $03.00 + .12

durability of adhesively bonded aluminium structures. One such procedure is to treat a Forest Products Laboratory (FPL) sodium dichromate/sulphuric acid etched adherend with certain organic acids (amino phosphonates) [8]. With a saturation inhibitor coverage of approximately one monolayer, these surfaces exhibit a much higher resistance to hydration (up to two orders of magnitude) than untreated FPL surfaces and have a corresponding increase in long-term bond durability [9].

In previous studies [6, 7, 9, 10], we have examined the mechanical properties of adhesive bonds formed with FPL and phosphoric acid anodized (PAA) adherends treated with hydration inhibitors, particularly nitrilotris methylene phosphonic acid (NTMP, $N[CH_2P(O)(OH)_2]_3$). We showed that: (i) NTMP-treated FPL bonds and PAA bonds exhibited similar long-term durability; (ii) the durability of NTMP-treated PAA bonds was better than that of untreated PAA bonds; and (iii) an inhibitor's effectiveness depended both on its ability to inhibit the oxide-to-hydroxide conversion and on its compatibility with the adhesive.

In this paper, we address the following issues: Why do inhibited aluminium oxide surfaces eventually hydrate? What causes failure of bonds made from inhibited adherends? What properties of an inhibitor are important in achieving good bond durability? To answer these questions we used X-ray photoelectron spectroscopy (XPS), supplemented with Fourier Transform Infra-red Spectroscopy (FTIR), to examine both the adsorption of NTMP and similar inhibitors onto FPL-prepared adherends and the hydration behaviour of the inhibited surfaces. Using the model for hydration thus developed, we modified the inhibitor molecule and performed wedge tests using adherends treated with these modified inhibitors. Based on the relative performance of the wedge-tested bonds and on a failure analysis of the aluminium panels, we have identified five important characteristics determining the effectiveness of inhibitors in improving bond durability.

2. Experimental procedure

2.1. Surface preparation

Test coupons and panels of bare 2024 Al were degreased by a 15 min immersion in an agitated solution of Turco 4215* (44 g l^{-1}) at 65° C and then rinsed in distilled, deionized water. Degreasing was followed by a standard FPL treatment [1], consisting of a 15 min immersion in an agitated aqueous solution of sodium dichromate dihydrate (60 g l^{-1}) and sulphuric acid (17 vol%) held at 65° C, after which samples were rinsed in distilled, deionized water and air dried. Some FPL-treated panels were then treated using the PAA process [2]. These panels were anodized in a 10 wt% phosphoric acid solution at a potential of 10 V for 20 min, rinsed in distilled, deionized water, and air dried.

The coupons were immersed for 30 min in a dilute aqueous solution of the inhibitor held at room temperature. Solution concentrations ranged from 0.1 to 500 ppm for the adsorption experiments and from 100 to 300 ppm for the hydration studies and wedge tests. In a separate experiment, the time of immersion of FPL surfaces in a 300 ppm NTMP solution was varied from 5 sec to 30 min. The samples were then thoroughly rinsed in distilled deionized water, forced-air dried, and stored in a desiccator until analysis.

Samples used in the hydration experiments were suspended vertically in a humidity chamber and exposed to air saturated with water vapour at 50° C. The samples were removed at different intervals, dried with forced air, and also stored in a desiccator.

Panels for wedge tests (6 in. × 6 in. × 0.125 in.) were bonded together using American Cyanamid FM 123-2 epoxy adhesive cured at 120° C and 40 psi† for 1 h. The bonded panels were cut into 1 in. × 6 in. test strips and a wedge (0.125 in. thick) was inserted between the two adherends to provide a stress at the bond-line. After 1 h equilibration at ambient conditions, the wedge-test samples were placed in a humidity chamber held at 60° C and 98% r.h. In order to determine the extent of crack propagation, the test pieces were periodically removed from the humidity chamber and examined under an optical microscope to mark the position of the crack front. When the test was complete, usually after 150 to 160 h, calipers were used to measure the positions of these marks, which determine crack length as a function of time.

*An alkaline cleaning agent manufactured by Turco Products, Los Angelos, California, USA.

†1 psi ≈ 6.894 kPa.

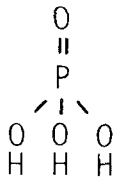

Phosphoric Acid[a]
[PA]

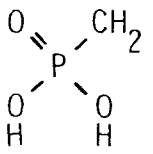

Methylene
Phosphonic Acid[a]
[MP]

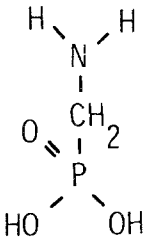

Amino Methylene
Phosphonic Acid[a]
[AMP]

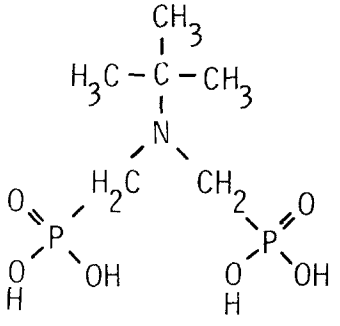

(t Butyl) Nitrilobis
Methylene Phosphonic Acid[b]
[(t Bu) NBMP]

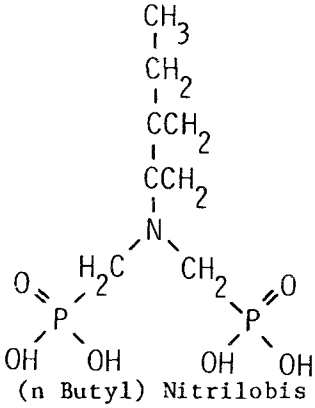

(n Butyl) Nitrilobis
Methylene Phosphonic Acid[b]
[(n Bu) NBMP]

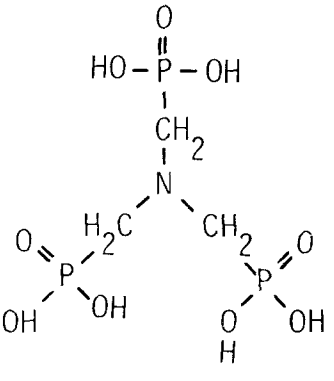

Nitrilotris Methylene
Phosphonic Acid[a] [NTMP]

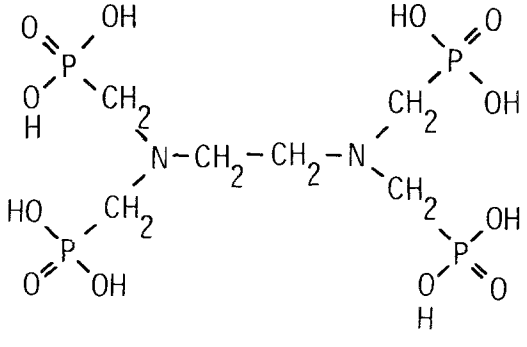

Ethylene Diamine Tetramethylene
Phosphonic Acid[b] [EDTMP]

Figure 1 Inhibitors tested: (a) denotes compounds commercially available and (b) denotes compounds synthesized.

2.2. Inhibitor selection and preparation

Each of the seven compounds shown in Fig. 1 was selected to investigate various aspects of the inhibitor process. NTMP serves as our standard. Ethylene diamine tetramethylene phosphonic acid {EDTMP, $[-CH_2N[CH_2P(O)(OH)_2]_2]_2$} increases the potential bonding sites to the aluminium oxide surface (POH groups) from six to eight. The inhibitor (n-Butyl) nitrilobis methylene phosphonic acid {(n Bu)NBMP: $CH_3(CH_2)_3N[CH_2P(O)(OH)_2]_2$} decreases the potential bonding sites to four, but exposes an extended hydrophobic end for possible

micromechanical interlocking with the adhesive. The inhibitor (t Butyl) nitrilobis methylene phosphonic acid {(t Bu)NBMP, $(CH_3)_3C-N[CH_2P(O)(OH)_2]_2$} also decreases the potential adsorbate-surface bonds to four, but is expected to expose a bulky hydrophobic end to the adhesive or aqueous environment. The remaining inhibitors – amino methylene phosphonic acid [AMP, $H_2NCH_2P(O)(OH)_2$,], methylene phosphonic acid {MP, $CH_3P(O)(OH)_2$} and phosphoric acid [PA, $P(O)(OH)_3$] – represent smaller sections of the NTMP molecule or, in the case of PA, an analogy to the phosphoric acid anodized (PAA) surface without its more complex morphology [3].

Four of the inhibitors investigated – NTMP, AMP, PA and MP – are commercially available; the others were synthesized according to the methods of Plaza [11]. Melting point measurements for these compounds were within the ranges previously reported [11]. Elemental analyses were close to the calculated values; in some cases intermediate products with fewer phosphonic acid groups may also have been present in small amounts.

2.3. Surface analysis

The surface composition of treated coupons was determined by XPS. Measurements were made on a Physical Electronics Model 548 spectrometer, which consists of a double-pass cylindrical mirror analyser (CMA) with pre-retarding grids and a coaxial electron gun, a magnesium anode X-ray source, a rastering 5 keV sputter ion gun, a sample introduction device, and a gas-handling system used to back-fill the chamber to 5×10^{-5} torr argon. Operating pressure was in the low 10^{-9} torr range. The XPS measurements were sometimes supplemented by Auger electron spectroscopy (AES) and ion sputtering to obtain an elemental distribution with depth.

Atomic concentrations were determined from high-resolution (50 eV pass energy) XPS spectra of the O 1*s*, Al 2*p*, and P 2*p* peaks [12]. The results were interpreted with the use of surface behaviour diagrams (SBDs) [12, 13], a recently developed method for analysing quantitative surface-sensitive results. These diagrams resemble ternary or quaternary phase diagrams in that they represent the surface composition as the sum of the compositions of three or four basis compounds. They differ, however, in that they display compositional data rather than structural data. In addition, the equilibrium condition is relaxed for SBDs, so that the surface can be described during non-equilibrium processes such as hydration. To this end, the SBDs graphically display the changes in the surface composition as a function of reaction time, solution concentration, anodization voltage, depth in the sample, or other parameters of interest. The measured changes can then be compared to those predicted by various models during analysis of the results.

In this study, the atomic concentrations of oxygen, aluminium and phosphorus were usually converted to molar concentrations of Al_2O_3, inhibitor, and H_2O using the following assumptions. All the phosphorus was assigned to the inhibitor, the aluminium was assigned to Al_2O_3, and enough oxygen was used to satisfy the inhibitor and Al_2O_3 stoichiometric requirements. Any excess oxygen was assumed to be bonded to hydrogen as H_2O. For example, AlOOH has a composition equivalent to $Al_2O_3 + H_2O$ even though it is not a two-phase mixture of these compounds. The molar concentrations were then plotted on the appropriate SBD. In certain cases, the atomic concentrations were also directly plotted onto an Al–P–O SBD.

Additional measurements were obtained from FTIR with a Nicolet 7199 spectrometer using the diffuse reflectance (DRIFT) technique. The samples were mixtures of the material of interest and KBr powder.

In some cases, wedge-test specimens were pulled apart following exposure to high humidity, and the near-crack-tip regions were examined by XPS or ultra-high resolution scanning electron microscopy (X-SEM) using a JEOL 100CX STEM to determine the locus of failure during the humidity exposure. Prior to examination by X-SEM, the samples were coated with an extremely thin vacuum-evaporated Pt–Pd coating to reduce charging, but without obscuring the fine structure present on FPL surfaces [3].

3. Results

3.1. Adsorption

The adsorption of NTMP on FPL surfaces was studied as a function of solution concentration and immersion time. The dependence of the surface coverage and composition on solution concentration is shown in the adsorption isotherm (Fig. 2) and in the Al_2O_3–NTMP–H_2O surface behaviour diagram (Fig. 3). In the SBD, the

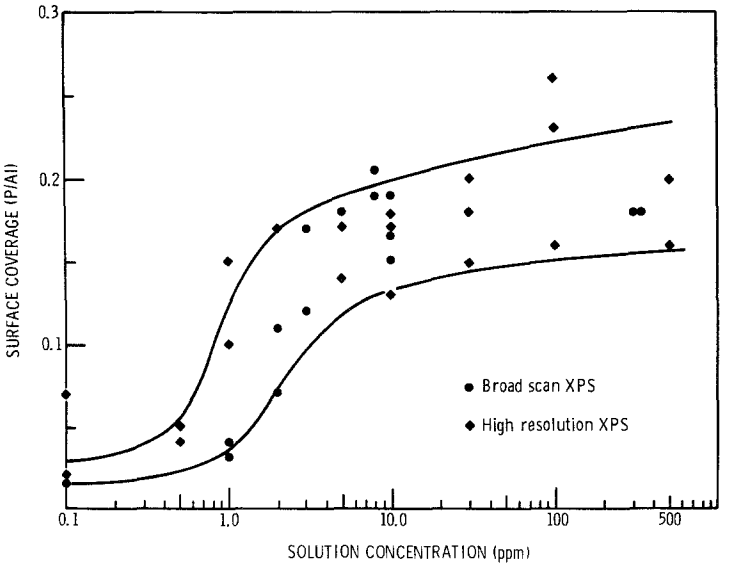

Figure 2 NTMP coverage (P/Al) of FPL-etched surfaces as a function of solution concentration [7].

solution concentration increases from left to right. The approximately horizontal position of the curve corresponds to the saturation coverage of P/Al $\approx$ 0.15 observed in Fig. 2. The adsorption process can be described as the displacement by NTMP of water or hydroxyl groups initially bound to the aluminium oxide surface. If the water were not removed during adsorption, the surface composition would evolve along a path directly toward the inhibitor.

NTMP saturation coverage on FPL surfaces is rapidly achieved on immersion. Fig. 4 indicates that the NTMP layer grows to monolayer thickness in less than 5 sec and remains at this level even after a 30 min (1800 sec) immersion.

Similar adsorption studies on the effect of solution concentration were done for AMP and (n Bu)NBMP on FPL. The adsorption of the two inhibitors (Figs. 5 and 6) are qualitatively similar to that of NTMP on FPL, i.e. a displacement reaction of the inhibitor in exchange for adsorbed water. Subtle differences between the NTMP and AMP adsorption behaviour, which are reflected in the different evolutionary paths in the Al–P–O elemental SBD shown in Fig. 7, will be discussed later.

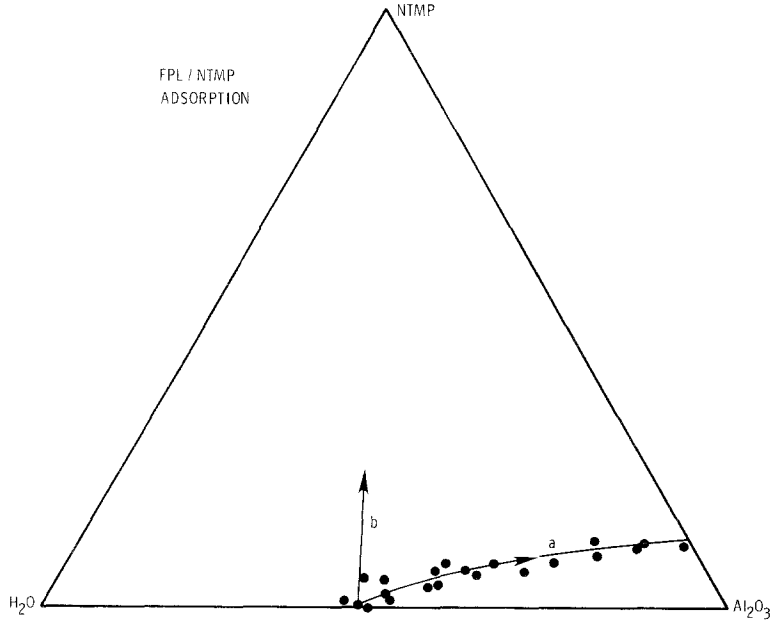

Figure 3 Al_2O_3–NTMP–H_2O SBD showing: (a) surface composition of FPL-etched surfaces after 30 min immersion in aqueous solutions of NTMP at concentrations ranging from 0.1 to 500 ppm, solution concentration increases from left to right; and (b) path representing no displacement of water.

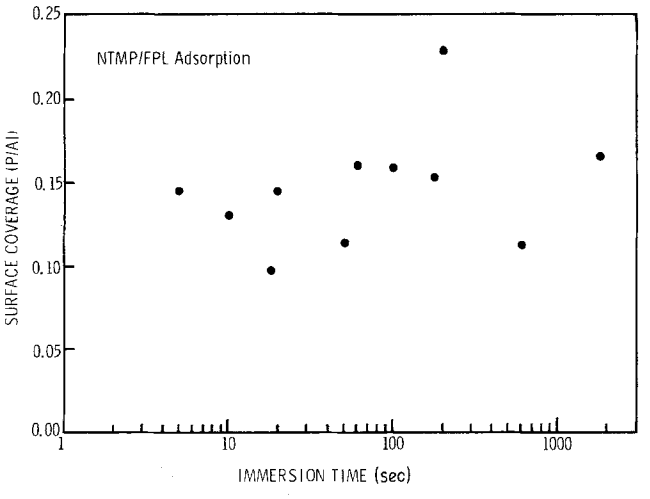

Figure 4 NTMP coverage (P/Al) of FPL-etched surfaces as a function of immersion time in a 300 ppm NTMP solution.

The FTIR spectrum of solid NTMP is shown in Fig. 8a, and the assignments of the various peak absorbances are given in Table I. Because of the high degree of symmetry in the molecule, the infra-red spectrum is very weak and comprises broad bands. Analysis of the FTIR results and determination of the bonding between NTMP and the aluminium surface was facilitated by studying the DRIFT spectrum of an Al–NTMP complex formed by reacting $Al(NO_3)_3$ with NTMP in a 2:1 molar ratio [15] (Fig. 8b and Table I). Significant changes in the P=O and P–O bonds (1200 to 700 cm^{-1}) are evident. The formation of an Al–O–P bond is indicated by the band at 956 cm^{-1} as well as by the shift to lower wavenumbers of the PO_3^{2-} group. Additional evidence is seen in that the P=O bond for Al–NTMP is much sharper than that for NTMP, indicating a decrease of symmetry on the PO_3^{2-} group. By analogy, we can conclude that the NTMP molecule adsorbs to the aluminium oxide surface via the initially present POH groups of the phosphonic acid.

3.2. Hydration

The hydration of NTMP-treated FPL surfaces in 100% r.h. at 50° C has also been investigated using XPS and SBDs. As shown in Fig. 9, the hydration path proceeds from an NTMP-covered Al_2O_3 surface to a boehmite [AlOOH] surface (line "a") and then to one of bayerite [$Al(OH)_3$]. Variation

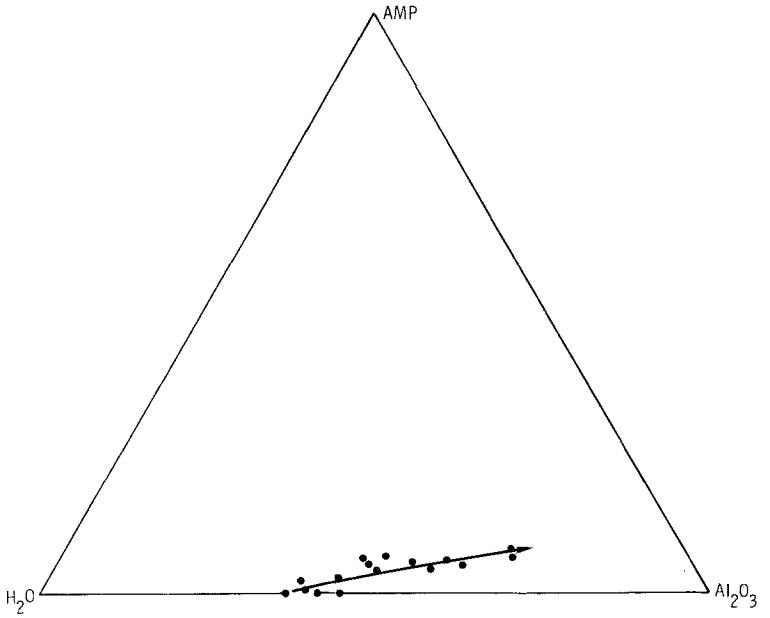

Figure 5 Al_2O_3–AMP–H_2O SBD showing the surface composition of FPL-etched surfaces after immersion in solutions of AMP at concentrations of 1 to 300 ppm.

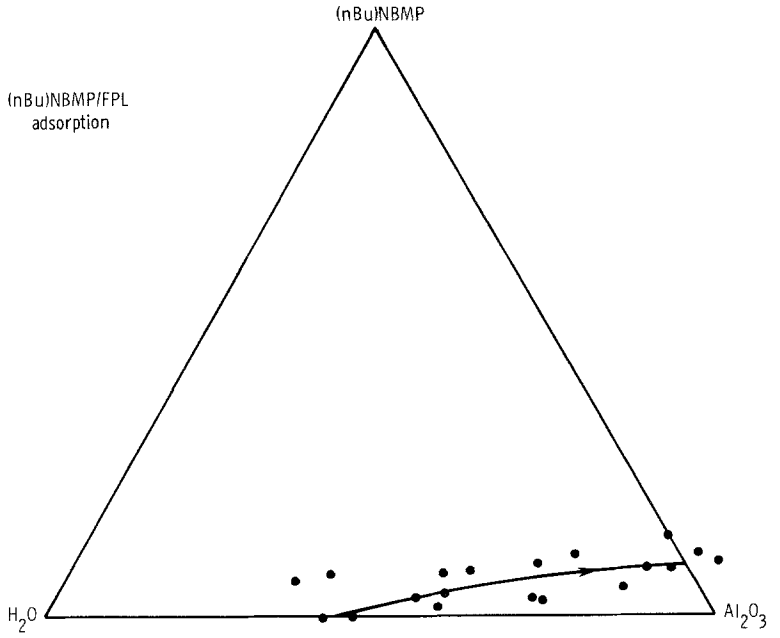

Figure 6 Al_2O_3–(n Bu)NBMP–H_2O SBD showing the surface composition of FPL-etched surfaces after immersion in solution of (n Bu)NBMP at concentrations of 1 to 300 ppm.

in this data is caused by physisorbed water [12, 14], represented by line "b", which was calculated by the addition of approximately one monolayer of water to surface compositions along line a. Surfaces with compositions along line b lost this physisorbed water after several days exposure to ultra-high vacuum (UHV), so that their final composition was near line a. Finally, Auger depth profiles of several samples revealed no subsurface concentration of phosphorus for coupons without surface phosphorus.

Similar hydration behaviour is also observed for FPL surfaces treated with (n Bu)NBMP. The surface again evolves directly from Al_2O_3 with a monolayer of inhibitor to AlOOH, and then to $Al(OH)_3$.

3.3. Wedge tests

Wedge tests were performed with FPL adherends treated with NTMP and several variants shown in Fig. 1.

From the results shown in Figs. 10 to 12, we

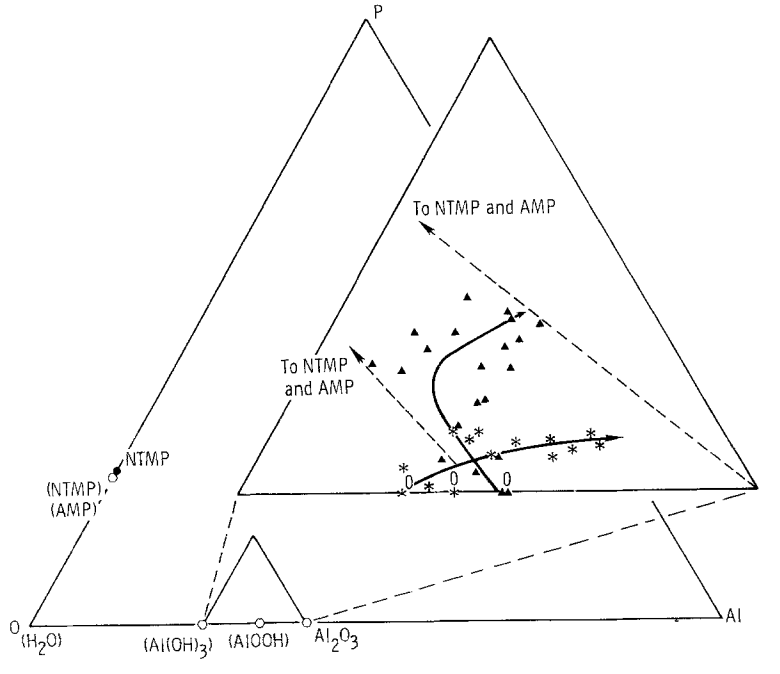

Figure 7 Al–P–O SBD showing the surface composition of FPL-etched surfaces after immersion in solutions of NTMP (▲) or AMP (☆) at various concentrations. Open hexagons (⬡) are calculated compositions. Compositions denoted by "0" represent surfaces not immersed in NTMP solutions.

TABLE I FTIR band assignments

Assignment	Wave numbers (cm^{-1})	
	NTMP	Al-NTMP
OH	3500-2800	3500-2800
NH^+	3020	3026
OH	1653	1646
CH_2	1435	1435
P=O	1188-970	1160
Al–O		956
PO_3^{2-}	808-723	
P–O–Al		751

can classify the inhibitors into three groups: (I) MP and PA, which provide either worse performance or no improvement over the untreated FPL specimens; (II) AMP and (t Bu)NBMP, which provide some improvement over the control; and (III) NTMP, (n Bu)NBMP, and EDTMP, which provide the best performances. In each case, however, the performance is not as good as that limited by the adhesive [7] (Fig. 10).

To determine the locus of failure of the wedge-test specimens, X-SEM micrographs and/or XPS

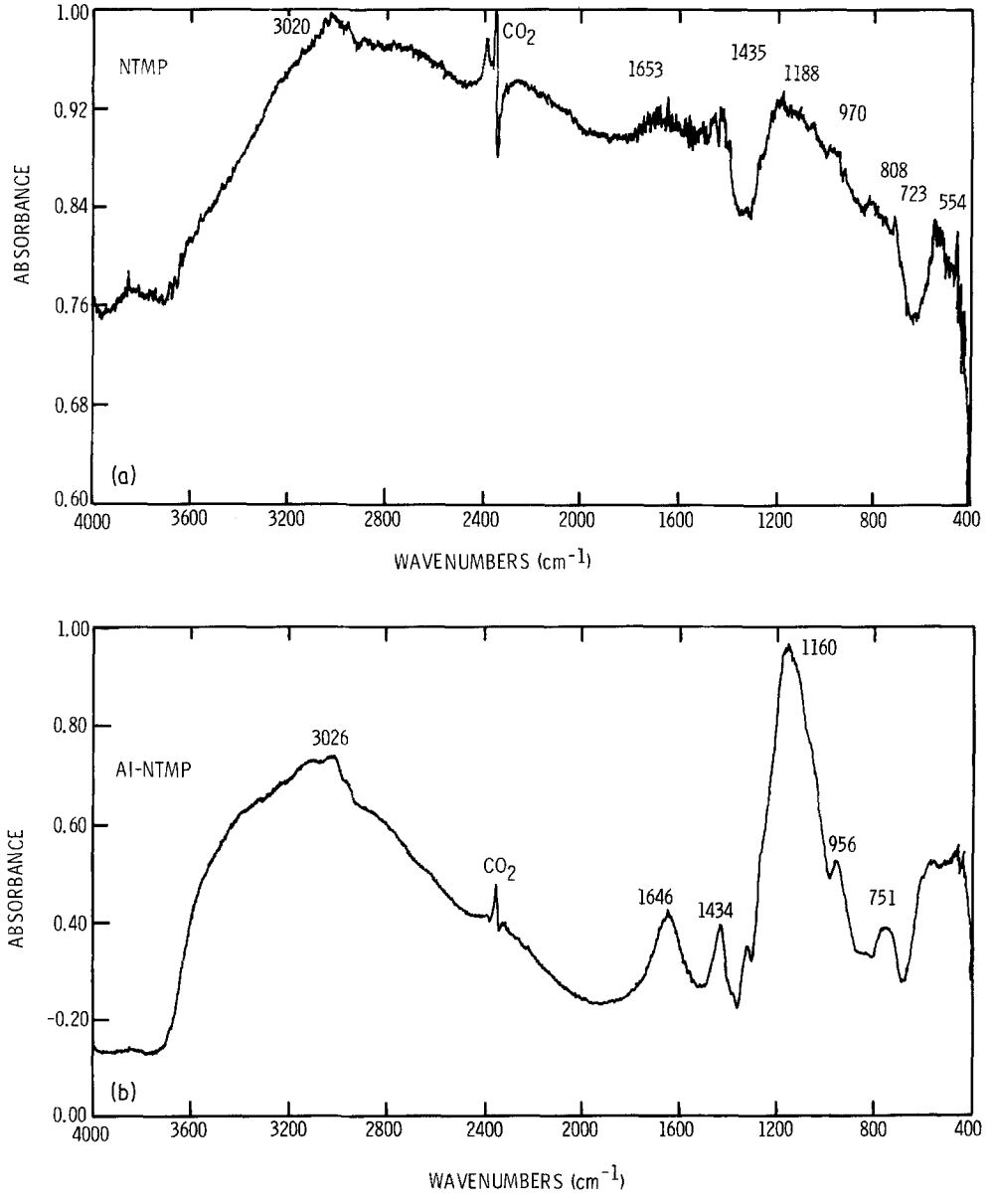

Figure 8 FTIR DRIFT spectrum of: (a) dried NTMP and (b) Al–NTMP complex.

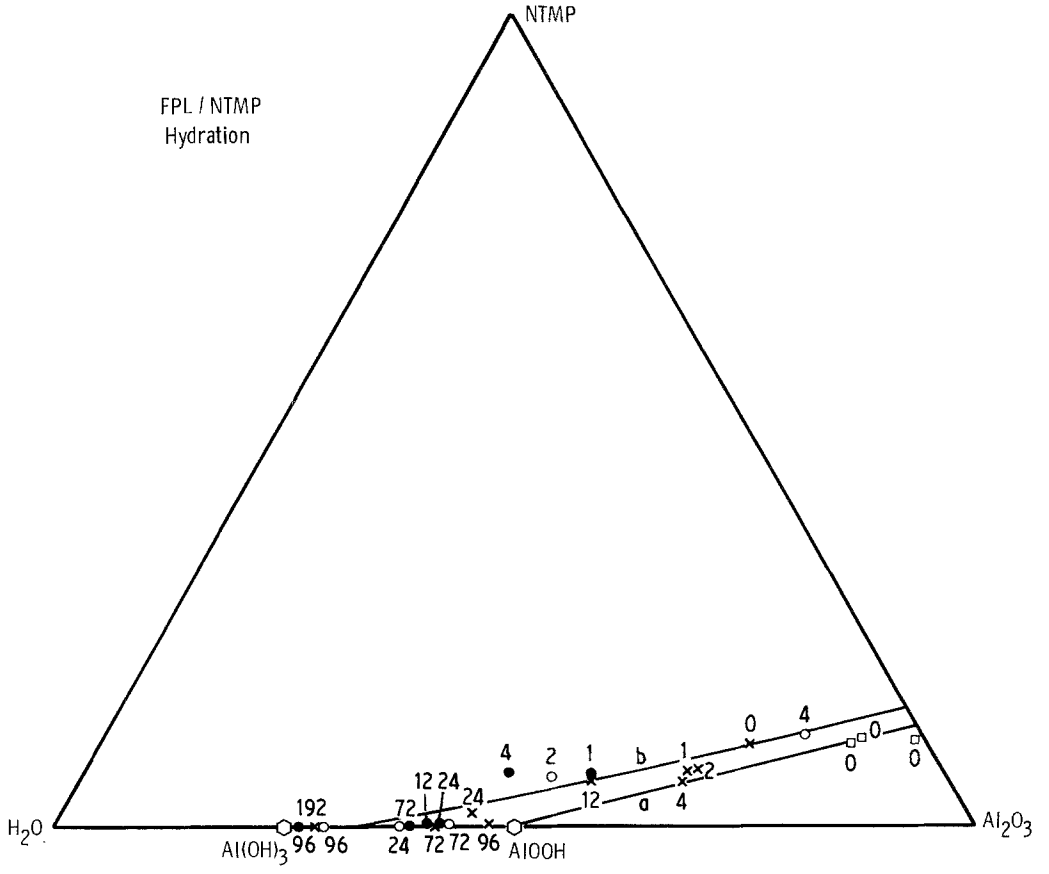

Figure 9 Al_2O_3–NTMP–H_2O SBD showing the evolution of the surface composition of FPL-etched surfaces treated with saturation coverages of NTMP, as a function of exposure time in 100% r.h. at 50° C. The different symbols represent different experimental runs; the numbers are the exposure time (h).

measurements of the near-crack-tip region were obtained for selected samples in each of the three groups. The XPS results are summarized in Table II. The failure of MP-, PA-, NTMP-, and EDTMP-treated specimens occur near or at the adhesive–adherend interface because substantial differences are seen between the metal and adhesive sides of the failure with high aluminium (and oxygen) denoting aluminium oxide or hydroxide and high carbon denoting the adhesive. (Aluminium and some oxygen on the adhesive side of NTMP- and EDTMP-treated bonds result from aluminium hydroxides solution-deposited from the condensed water vapour. Similarly the carbon on the metal side results from adventitious hydrocarbon contamination.) In contrast, the two surfaces of the FPL control and specimens treated with (t Bu) NBMP and (n Bu)NBMP exhibit high aluminium and oxygen and low carbon, indicating that the locus of failure is in the oxide/hydroxide or at the interface between the oxide/hydroxide and the metal with subsequent hydration or corrosion of the metal surface. For all cases, because the failures are not cohesive in the adhesive, further improvement in the bond performance may be possible using other inhibitors.

TABLE II Surface composition of failed surfaces (at %)

Group	Inhibitor	Al		O		C	
		M*	A†	M	A	M	A
	Adhesive	–	0	–	8	–	92
	Control	22	24	44	47	34	30
I	MP	20	0	50	21	29	78
I	PA (66 ppm)	25	2	49	25	25	73
II	(t Bu)NBMP	30	29	59	58	10	12
III	NTMP	30	14	56	38	13	47
III	EDTMP	29	19	59	45	12	36
III	(n Bu)NBMP	31	30	56	58	13	11

*Metal side.
†Adhesive side.

The micrographs of the near-crack-tip region of NTMP-treated panels reveal a "shiny" aluminium area right at the crack tip and a "dull" region further along the crack (Fig. 13). Closer

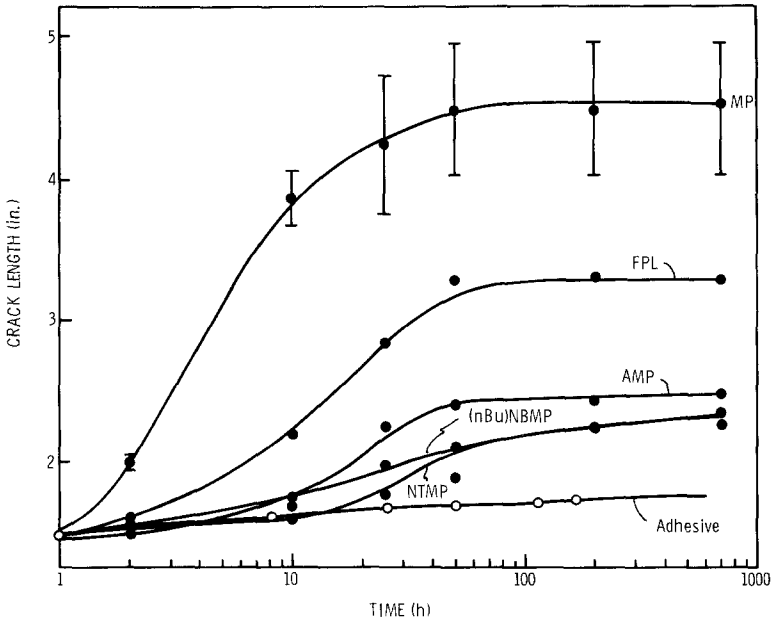

Figure 10 Wedge-test results (crack length as a function of time) for FPL adherends treated in solutions of MP, AMP, (n Bu)NBMP, and NTMP and for untreated FPL adherends. Also shown is the limiting performance of bonds made with FM 123-2.

examination shows the shiny area to exhibit an FPL morphology while the dull area exhibits the cornflake morphology of a hydrated surface [3]. In this case, the crack has apparently propagated in advance of the hydration of the aluminium oxide; only after additional exposure to the moist environment does hydration occur.

In other specimens that show improvement over the control, bond failure apparently occurred as a result of hydration. This hydration is demonstrated in Fig. 14, which shows the crack-tip region of panels treated with AMP and (n Bu) NBMP. Here cornflake morphology is present up to the crack tip. In some areas, more extensive hydration is also seen with bayerite crystallites on top of the boehmite.

4. Discussion

4.1. Adsorption

The adsorption of each of the three amino phosphonates studied proceeds by the displacement of the physisorbed water on the FPL surface. (This

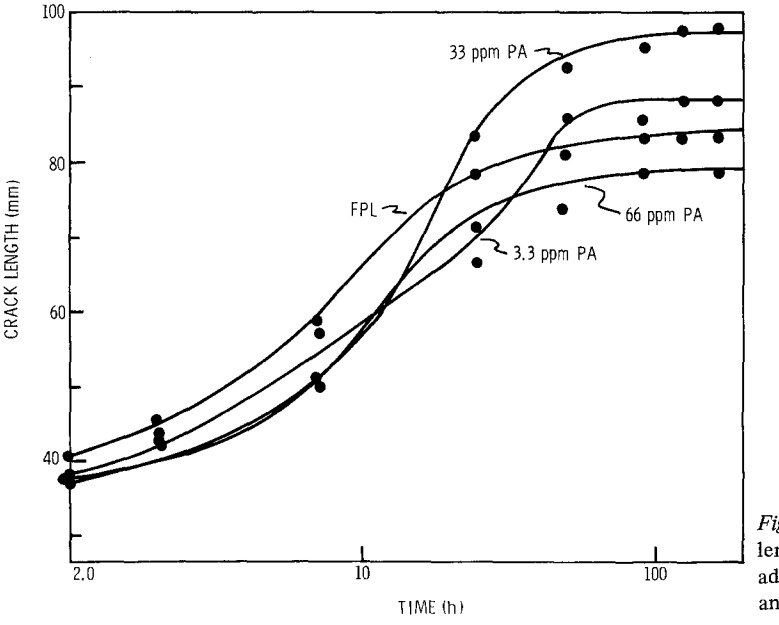

Figure 11 Wedge-test results (crack length as a function of time) for FPL adherends treated in solutions of PA and for untreated FPL adherends [7].

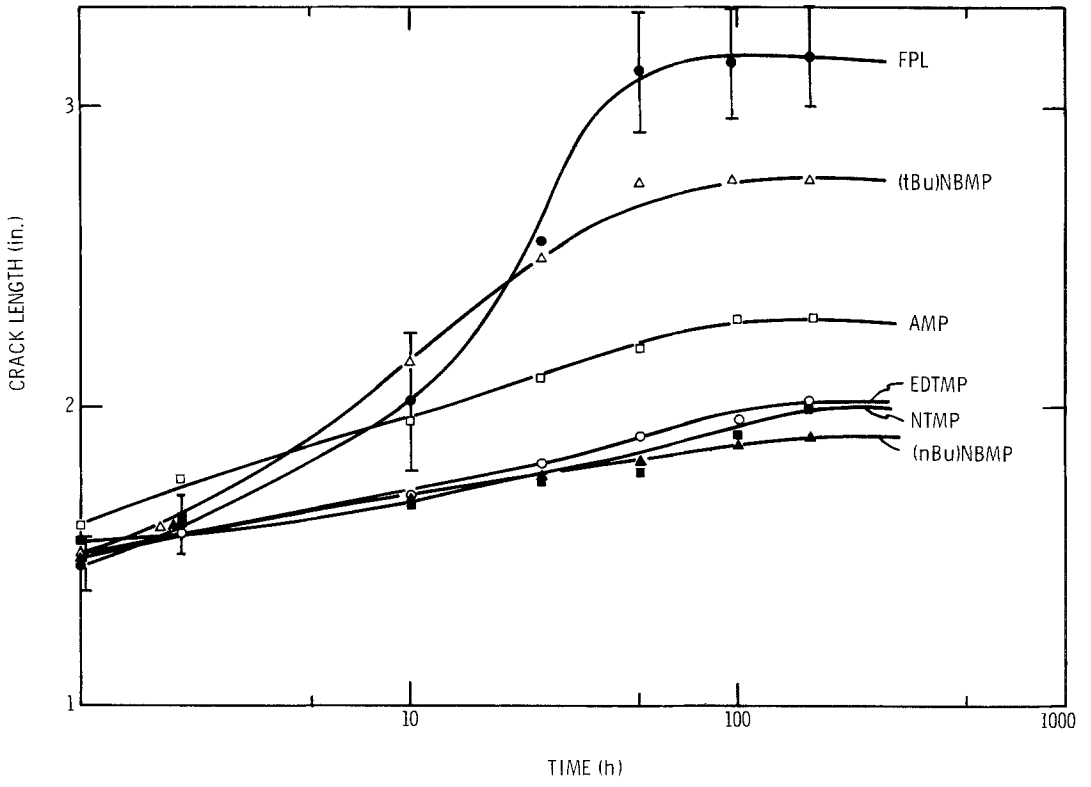

Figure 12 Wedge-test results (crack length as a function of time) for FPL adherends treated in solutions of AMP, (n Bu)NBMP, (t Bu)NBMP, NTMP, and EDTMP, and for untreated FPL adherends.

water can also be removed by storing the coupon in UHV for several days, the surface, however, regains the water upon exposure to normal humid atmosphere.) For NTMP and (n Bu)NBMP this reaction continues at room temperature until most, if not all, physisorbed water is replaced by approximately one monolayer of chemisorbed inhibitor. However, it appears that AMP is less efficient at displacing physisorbed water, so that some water remains even at the highest AMP coverages achieved at room temperature. This presence of residual water is consistent with the lower phosphorus content on the surface at saturation [9]. Our model of adsorption suggests one phosphorus atom for every two water molecules removed from the surface (assuming that all the inhibitor's POH groups bond to the Al_2O_3). Since the AMP-treated surface has a significantly lower P/Al ratio, less water would have been displaced from the surface.

The adsorption data of NTMP on FPL (Fig. 3) show the adsorption isotherm to be concave downward. This is indicative of a two-step adsorption process more clearly illustrated in Fig. 7, which shows the isotherm proceeding at first in the general direction of NTMP, but then heading away from the H_2O vertex. These results suggest that at very low solution concentrations, NTMP adsorbs with only one PO_3^{2-} group bonded to the surface. Consequently the inhibitor coverage, as determined by the amount of phosphorus on the surface, increases more quickly than the water concentration on the surface decreases. At higher concentrations, however, the NTMP competes more successfully with water for adsorption sites, and the other PO_3^{2-} groups of the molecule become bonded to the surface, displacing additional water without increasing the inhibitor coverage.

A similar two-step process is expected for (n Bu)NBMP adsorption on FPL, although a single-step process is expected for AMP, since it has only one phosphonic acid group per molecule. The SBDs shown in Figs. 5, 6, and 7 support these ideas. Fig. 7 clearly shows only a slight curvature in the surface composition evolutionary path for AMP on FPL, in contrast to the distinct two-step adsorption process for NTMP on FPL.

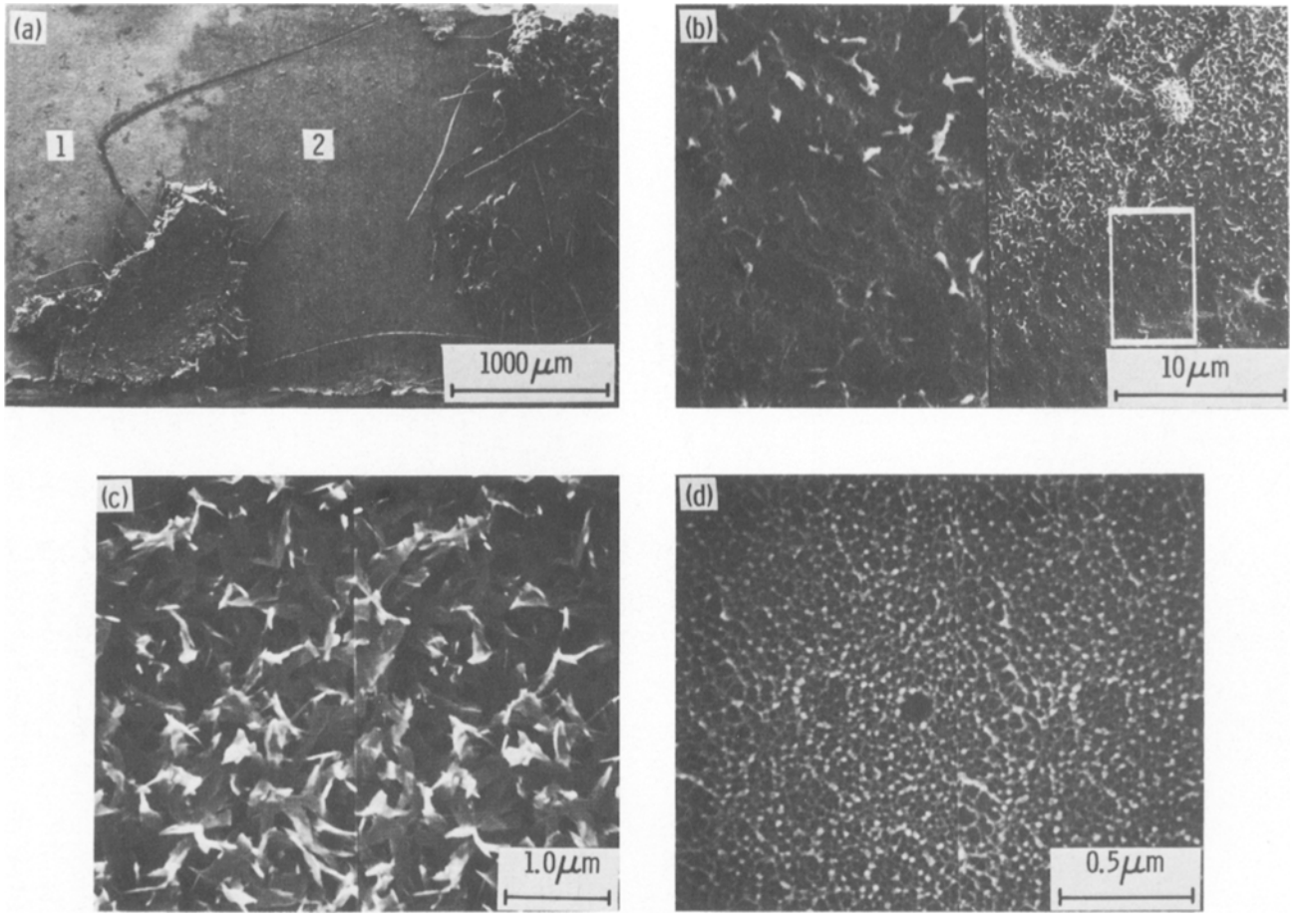

Figure 13 Scanning electron micrographs of the near-crack-tip region of the aluminium side of an NTMP-treated FPL-etched wedge-test specimen: (a) low magnification view showing 1. the "dull" aluminium area and 2. the "shiny" aluminium area, and the cohesive failure in the adhesive after the wedge test was completed (at right); (b) the beginning of hydration in the boundary region between dull and shiny areas, enlargement of the blocked-in area in inset is at left; (c) higher magnification stereo view of the dull area showing the cornflake boehmite structure; and (d) high magnification stereo view of the shiny area showing the original FPL morphology.

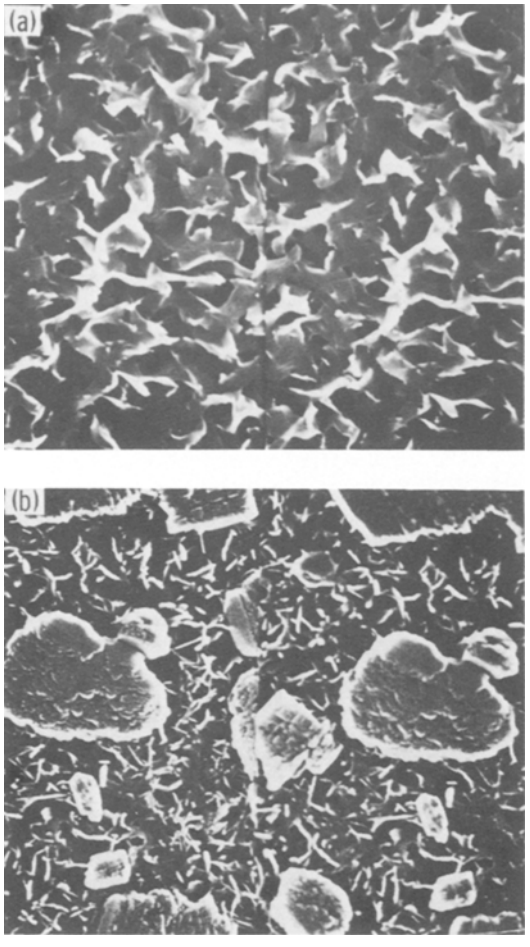

Figure 14 Scanning electron micrographs of the near-crack-tip region of the aluminium side of two inhibitor treated FPL-etched wedge-test specimens: (a) AMP-treated surface exhibiting cornflake (boehmite) morphology, and (b) (n Bu)NBMP-treated surface exhibiting bayerite crystallites on top of boehmite.

4.2. Hydration

The behaviour of the surface composition during the hydration of NTMP-treated FPL surfaces (Fig. 9) is very similar to that observed during the hydration of PAA surfaces [12]. First, a reversible physisorption of water occurs. Then the surface hydrates to boehmite. Finally, bayerite crystallites grow on top of the boehmite. In fact, the linear evolutionary path of the surface composition from the monolayer of NTMP on Al_2O_3 to boehmite, together with the absence of any subsurface phosphorus in the hydration product, indicates that hydration only occurs as the NTMP-aluminium complex dissolves from the surface. Apparently, the limiting step in the hydration is the dissolution of this complex.

These findings, which have been generalized to include the corrosion of NTMP-treated steel samples [14] as well as the hydration of PAA surfaces [12], suggest that at an ideal inhibitor should: (i) displace water and occupy all the active sites on the surface; (ii) bond strongly to the surface; and (iii) form an insoluble complex with aluminium.

4.3. Wedge tests

Wedge test results allow us to identify two additional properties of an ideal inhibitor. Treatment with MP accelerates bond failure compared to FPL adherends while treatment with PA provides no change in performance even though it does confer hydration-resistance to the unbonded surface [16]. For both bonds, the crack propagated along the adhesive–oxide interface. The inhibitors, apparently weakened this interface, making it susceptible to attack by moisture either by interfering with the curing of the epoxy adhesive at the surface or by passivating the adherend surface and preventing the formation of adhesive–oxide or adhesive–inhibitor chemical bonds. In either case, compatibility of the inhibitor with the adhesive is necessary to prevent rapid bond failure.

A final criterion for a good inhibitor – coupling to the adhesive – can be deduced from the micrographs of the crack-tip region and from the relative performance of adherends treated with the two (Bu)NBMP compounds. Samples treated with (t Bu)NBMP and AMP exhibit only moderate bond durability. Failure occurs as the oxide hydrates, leading to crack propagation within the hydroxide, or along the weak hydroxide–metal interface with subsequent hydration of the exposed metal surface.

Even treatment with (n Bu)NBMP, although it gives good bond durability, leads to failure by hydration. We attribute the improved performance of these samples over those treated with (t Bu) NBMP to a molecular mechanical interlocking or good dispersion of the n-butyl tail in the polymeric adhesive. This mechanical coupling would make the inhibitor less vulnerable to aqueous attack and improve bond durability. It is not sufficient, however, to fully compensate for the reduced number of inhibitor–oxide bonds. As a result, treatment with (n Bu)NBMP fails to provide

superior performance to that of NTMP-treated adherends. A similar effect may occur with AMP-treated bonds. The addition of the amino group to MP makes a dramatic difference in the performance of the respective bonds. This amino group is capable of reacting with the epoxy adhesive, thus strengthening the inhibitor–adhesive interface. At the same time, by making a less soluble complex, the inhibitor probably increases the hydration resistance of the oxide, even though the water that remains on the surface can act as initiation sites for hydration. These initiation sites prevent the hydration resistance from becoming as high as that of NTMP-treated oxides.

The failure of the NTMP-treated specimens, on the other hand, occurs not upon hydration, but prior to hydration. In these cases, the hydration rate is slowed sufficiently so that it is no longer the limiting factor in bond durability. Instead, failure occurs along the inhibitor–adhesive interface, and only after subsequent exposure does the oxide surface hydrate. These results, then, suggest that further improvement in bond durability can be achieved by strengthening the inhibitor–adhesive interface by either chemical or mechanical coupling while maintaining strong inhibitor–oxide bonding.

5. Summary

We have investigated the mechanisms by which nitrilotris methylene phosphonic acid (NTMP) and related compounds adsorb onto oxidized aluminium surfaces, inhibit the hydration of this oxide, and increase the durability of adhesive bonds formed with inhibitor-treated panels. Our results indicate that:

1. NTMP adsorbs via P–O–Al bonds;

2. water initially adsorbed onto the FPL surface is displaced by the NTMP; and

3. hydration of NTMP-treated FPL surfaces occurs in three stages: (i) reversible physisorption of water; (ii) slow dissolution of NTMP followed by the rapid hydration of the freshly exposed Al_2O_3 to AlOOH, and (iii) further hydration of the surface to $Al(OH)_3$.

Additionally, by comparing the behaviour of wedge-tested panels treated with different inhibitors and by determining the locus of failure, we have identified five properties of an ideal inhibitor that can improve adhesive bond durability. The inhibitor should:

1. displace water from the surface and occupy all the active sites;

2. bond strongly to the surface;

3. form an insoluble complex with aluminium;

4. be compatible with the primer/adhesive system; and

5. chemically couple the adhesive to the oxide.

Acknowledgements

The authors gratefully acknowledge the valuable technical assistance of R. C. Butler, A. I. Desai, D. K. Shaffer, and T. K. Shah. This work was funded by ONR and ARO under contract N00014-80-C-0718.

References

1. H. W. EICHNER and W. E. SCHOWALTER, Forest Products Laboratory Report No. 1813, Madison, WI, (1950).
2. G. S. KABAYASKI and D. J. DONNELLY, Boeing Corporation Report No. D6-41517, Seattle, WA, (1974).
3. J. D. VENABLES, D. K. McNAMARA, J. M. CHEN and T. S. SUN, *Appl. Surf. Sci.* 3 (1979) 88.
4. D. J. PACKHAM, in "Adhesion Aspects of Polymeric Coatings", edited by K. L. Mittal (Plenum, New York, 1983) p. 19 and the references therein.
5. J. D. VENABLES, D. K. McNAMARA, J. M. CHEN, B. M. DITCHEK, T. I. MORGENTHALER and T. S. SUN, in Proceedings of the 12th National SAMPE Technical Conference, Seattle, WA, 1980, (SAMPE, Azuso, California, 1980) p. 909.
6. G. D. DAVIS and J. D. VENABLES, in "Durability of Structural Adhesives", edited by A. J. Kinloch (Applied Science, Essex, 1983) p. 43.
7. D. A. HARDWICK, J. S. AHEARN and J. D. VENABLES, *J. Mater. Sci.* 19 (1984) 223.
8. J. D. VENABLES, M. E. TADROS and B. M. DITCHEK, US Patent 4308 079, (1981).
9. J. S. AHEARN, G. D. DAVIS, T. S. SUN and J. D. VENABLES, in "Adhesion Aspects of Polymeric Coatings", edited by K. L. Mittal (Plenum, New York, 1983) p. 281.
10. D. A. HARDWICK, J. S. AHEARN and J. D. VENABLES (to be published).
11. A. I. PLAZA, PhD thesis, University of Maryland (1976) unpublished.
12. G. D. DAVIS, T. S. SUN, J. S. AHEARN and J. D. VENABLES, *J. Mater. Sci.* 17 (1982) 1807.
13. G. D. DAVIS, S. P. BUCHNER, W. A. BECK and N. E. BYER, *Appl. Surf. Sci.* 15 (1983) 238.
14. G. D. DAVIS, J. S. AHEARN and J. D. VENABLES, *J. Vac. Sci. Technol. A.* 2 (1984) 763.
15. S. S. MOROZOVA, L. V. NIKITINA, N. M. DYATIOVA and G. V. SEREBRYAKOVA, *Z. Anal. Khim.* 30 (1975) 1712.
16. J. S. AHEARN and A. I. DESAI, unpublished results.

Received 27 March
and accepted 10 May 1984